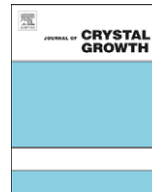




Contents lists available at ScienceDirect

Journal of Crystal Growth

journal homepage: [www.elsevier.com/locate/jcrysgr](http://www.elsevier.com/locate/jcrysgr)

# Al(In)As–(Ga)InAs strain-compensated active regions for injectorless quantum cascade lasers

Gerhard Boehm\*, Simeon Katz, Ralf Meyer, Markus-Christian Amann

Walter Schottky Institut, Technische Universität München, Am Coulombwall 3, 85748 Garching, Germany

## ARTICLE INFO

PACS:  
42.55.Px

Keywords:

A3. Laser epitaxy  
B1. Arsenates  
B1. Phosphides  
B2. Semiconducting III/V materials  
B3. Infrared devices  
B3. Laser diodes

## ABSTRACT

We present a new design for quantum cascade lasers (QCLs) without the typically used injector between two consecutive active stages. The lasers are realized with the InP-based material system AlInAs/GaInAs. With additional AlAs and InAs layers a significant optimization of the structure can be realized. In this improved structure the possibility of electrons escaping into the quasi-continuum is drastically reduced by the AlAs-blocking layer. On the other hand, InAs, a material with a very low effective mass, significantly prolongs the carrier lifetime, enhancing the population inversion and increasing the dipole matrix element of the transition. Both inserted layers result in an overall improvement of the device properties, basically the threshold current density ( $j_{th}$ ), maximum operating temperature ( $T_{max}$ ), output power, slope efficiency and characteristic temperature  $T_0$ . With high reflection coated facets a record threshold current density as low as 450 A/cm<sup>2</sup> at 300 K was achieved in the pulsed mode.

© 2008 Elsevier B.V. All rights reserved.

## 1. Introduction

Quantum cascade lasers (QCLs) are attractive light sources in the wavelength range from about 3 μm up to more than 100 μm and therefore suitable for applications like gas-sensing and optical free-space data communication. In this work an alternative design without an injector region is investigated with regard to an optimization concerning band structure, choice of material system and growth conditions [1].

The injector region in a standard QCL generally works as a moderator for the electron injection into the subsequent stage and reduces thermal backfilling of the lower laser level. Otherwise it is an optical inactive part within the active region and reduces significantly the confinement factor and is therefore detrimental to most of the relevant device parameters. For this reason in this work the injector is removed and the active stages are assembled together in a way that the ground level of one stage is in resonance with the upper laser level of the subsequent stage.

## 2. Device optimization

There are several design parameters affecting the active region, which influence directly the device performance. Apart from the thickness of the quantum wells, which mainly determines the emission wavelength, there are the length and number of stages,

doping level and location as well as the choice of the material system. On the other hand, we have device parameters as threshold current density ( $j_{th}$ ), maximum operating temperature ( $T_{max}$ ), output power, slope efficiency and characteristic temperature  $T_0$ .

To work out the relation between design and device parameter, two types of active regions are compared in this work. The reference structure [2] (Fig. 1a) consists of the strain-compensated material system Al<sub>0.6</sub>In<sub>0.4</sub>As/Ga<sub>0.4</sub>In<sub>0.6</sub>As grown on InP, and a new type of structure [3] with an additional AlAs-blocking layer and an InAs-layer in one of the quantum wells (Fig. 1b). In this improved structure, the possibility of electrons escaping into the quasi-continuum is drastically reduced by the AlAs-blocking layer [4,5]. On the other hand, the inserted InAs quantum well serves to significantly prolong the carrier lifetime and the dipole matrix element of the transition. With the insertion of these two layers the overall performance of the device should be improved.

## 3. Growth optimization

The layer structures were realized with a standard MBE system equipped with a valved phosphorous cell. The structures were grown on low-sulphur-doped InP substrates ( $n=6 \times 10^{16} \text{ cm}^{-3}$ ). Both types of active regions were designed for an emission wavelength of 6.8 μm, consisting of 60 stages and had a confinement factor of up to 0.6.

A critical value for the epitaxy is the accumulated strain in the active region (Fig. 2). First the thickness of the AlAs and InAs

\*Corresponding author. Tel.: +49 89 289 12791; fax: +49 89 3206 620.  
E-mail address: boehm@wsi.tum.de (G. Boehm).

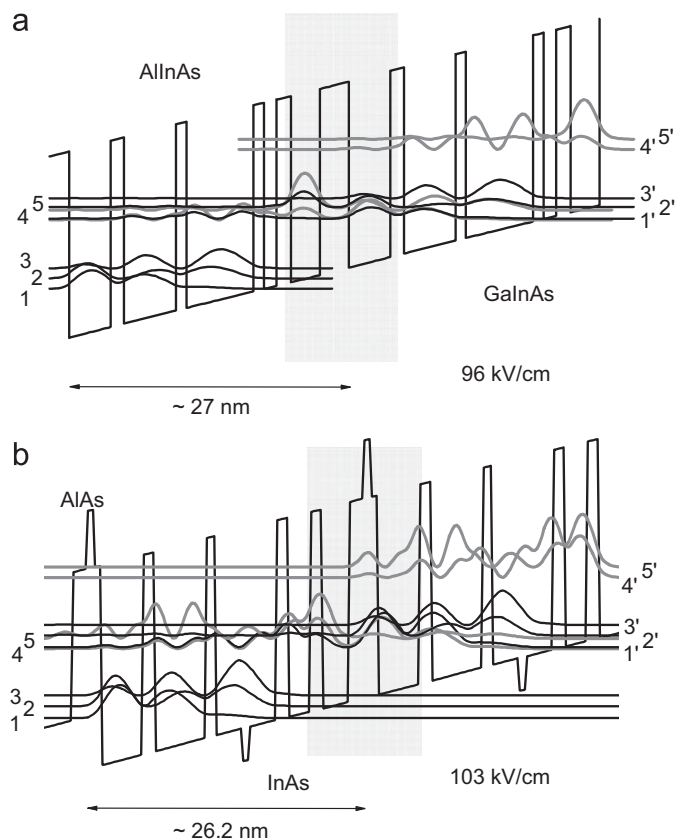


**Fig. 1.** Conduction band characteristics of two stages of the active region for the (a) standard design [2] operating at an electric field of 96 kV/cm, and (b) the new design [3] with AlAs blocking layer and InAs layer operating at 103 kV/cm. For both designs levels 1 and 2 of one stage are in resonance with levels 4 and 5 of the following stage. The laser transition takes place between levels 4 and 3 (black arrow). The grayed layers are doped.

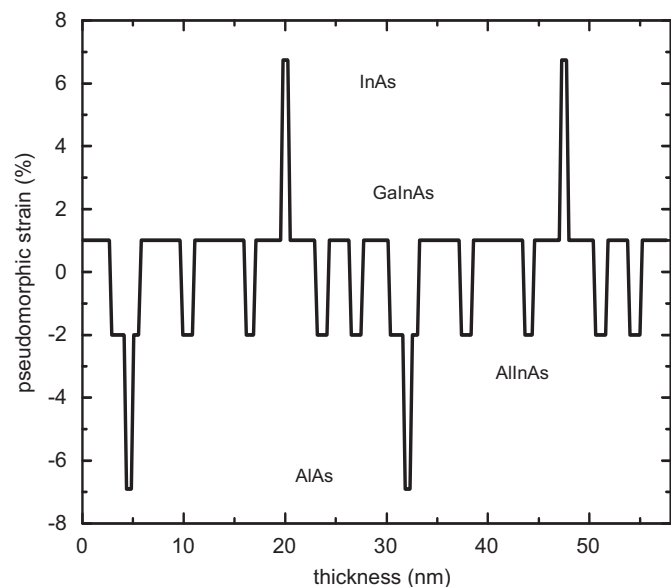


**Fig. 2.** Strain profile of one stage in the active region. Positive values indicate compressive strain, negative values tensile strain.

layers must not exceed the critical thickness. To prevent too much strain on the interfaces, both layers should not be grown directly on top of each other. Since the total thickness of the active region

adds up to more than 1  $\mu\text{m}$  (60 stages), one stage should be completely strain-balanced. If this requirement is fulfilled a relatively high growth temperature for the active region of 520  $^{\circ}\text{C}$  can be used. In contrast to this the growth temperature of the 2.5  $\mu\text{m}$  InP-cladding was set around 420  $^{\circ}\text{C}$ . Both structures, the reference and the new design, were completed with a 1- $\mu\text{m}$ -thick highly doped GaInAs contact layer. The doping level in the active region was varied from  $6.5 \times 10^{16}$  down to  $2.6 \times 10^{16} \text{ cm}^{-3}$ , the number of stages from 40 to 60 for the reference. The resulting doping sheet density varies from  $6.3 \times 10^{10}$  down to  $2.5 \times 10^{10} \text{ cm}^{-2}$ .

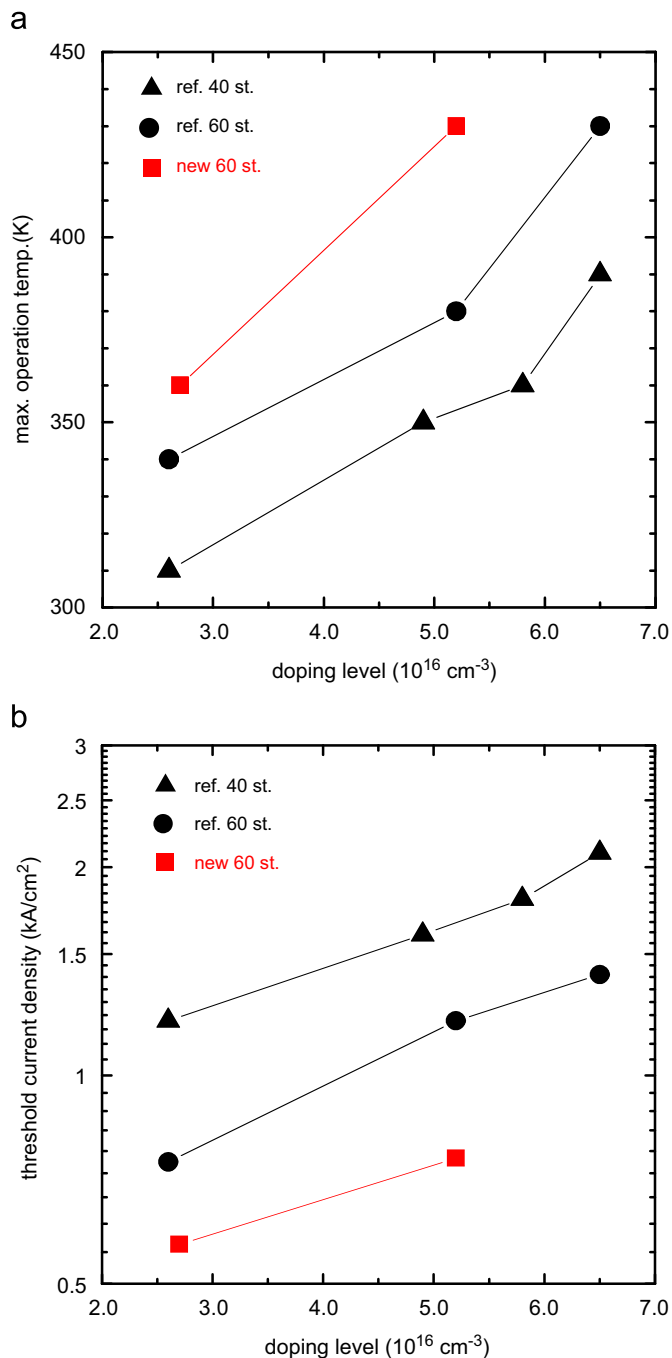


**Fig. 3.** Comparison of reference (40 and 60 stages) and new design (60 stages) concerning (a) threshold current density and (b) maximum operating temperature. All data were measured on devices with 4 mm length and 26  $\mu\text{m}$  stripe width measured at 300 K in the pulsed mode.

#### 4. Device performance

After growth, ridge-waveguide lasers with 4 mm length and a stripe-width of 26  $\mu\text{m}$  were fabricated. Device operation was measured in the pulsed mode using 250 ns pulses with a repetition rate of 250 Hz. Most of the devices had uncoated facets, except for some selected lasers, where a high reflection coating was deposited on the back facet while the front facet was left uncoated. The coating consisted of two pairs of ZnS–Si reflectors decreasing the mirror losses from 3.2 down to 1.8  $\text{cm}^{-1}$ .

Fig. 3a shows the dependency of maximum operation temperature and threshold current density versus doping level. Both parameters are decreasing with lower doping levels so that the optimized device will be a tradeoff between threshold current density and maximum operation temperature. On the one hand a higher doping level leads to higher population inversion, resulting in a higher maximum operation temperature, otherwise a lower doping level generates less losses, which leads to a reduced threshold current density (Fig. 3b).

With the removal of the injector part in the active region, the length of the stages is cut into halves and therefore the number of stages can be increased, resulting in a better confinement factor and leads therefore to an improvement of  $j_{\text{th}}$  and  $T_{\text{max}}$ . Both parameters are enhanced by increasing the number of stages from 40 to 60 (Fig. 3a and b), improving the confinement factor from 0.43 to 0.57. Devices with the new design (60 stages,  $\Gamma=0.54$ ) show for both dependencies ( $j_{\text{th}}$ ,  $T_{\text{max}}$  versus doping level, Fig. 3a and b) a large improvement compared with the reference. The AIAs layer improves  $T_{\text{max}}$  by reducing the probability for electrons escaping into the quasi-continuum and the inserted InAs-layer with its lower effective mass reduces significantly  $j_{\text{th}}$ .

The positive influence of the new design continues as well for the characteristic temperature  $T_0$ . Fig. 4 reveals a lower  $T_0$  (90 K) for the device with reference design compared with the new design (140 K). A further improvement concerning  $T_{\text{max}}$  and  $j_{\text{th}}$  shows the device with new design and high-reflection coating. All devices were realized with a doping level in the active region as low as  $2.6 \times 10^{16} \text{ cm}^{-3}$ . The threshold current density drops to 450  $\text{A}/\text{cm}^2$  at 300 K for the HR-coated device, which is a record value for all types of QCLs, while the threshold voltage reaches

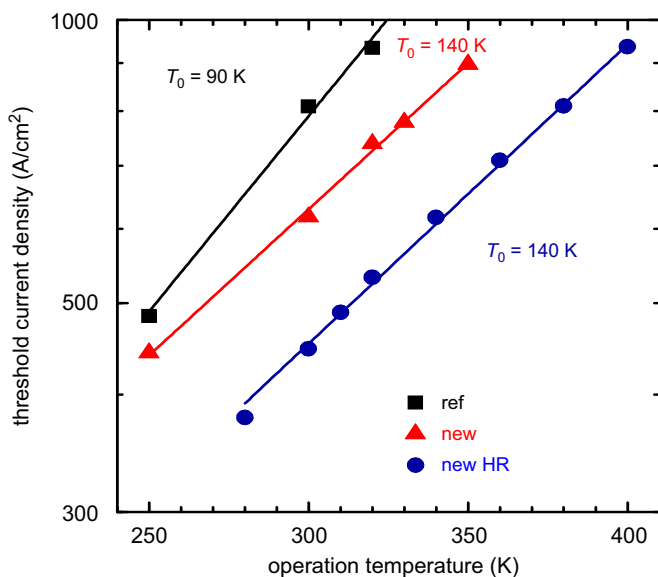


Fig. 4. Temperature dependence of the active region for reference design ( $T_0=90\text{K}$ ) and new design w/o high-reflection coating ( $T_0=140\text{K}$ ). The threshold current density is plotted versus the operation temperature. A threshold current density of 450  $\text{A}/\text{cm}^2$  at 300 K for the HR-coated device is a record value for all types of QCLs.

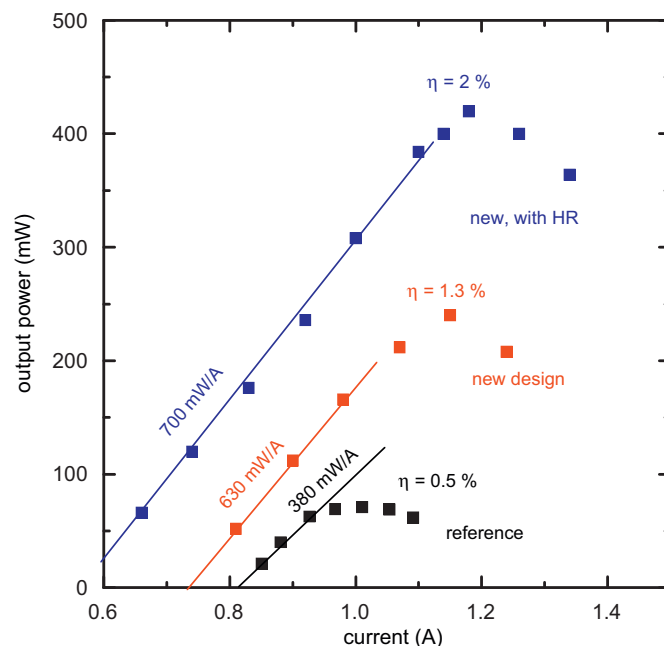


Fig. 5. Output power versus current, slope efficiency and conversion efficiency of the device for reference design and new design w/o high-reflection coating.

13 V. Fig. 5 shows a comparison of reference and new design concerning output power ( $P_{\text{max}}$ ), slope efficiency and front facet wall plug efficiency. Again a clear improvement of the new design is observable. All three device parameters are enhanced ( $P_{\text{max}}$  from 70 to 240 mW, slope efficiency from 380 to 630  $\text{mW}/\text{A}$  and conversion efficiency from 0.5% to 1.3%). With high-reflection coating the device parameters show once more even better values, 420 mW, 700  $\text{mA}/\text{W}$  and 2% for maximum output power, slope efficiency and front facet wall plug efficiency, respectively.

#### 5. Conclusion

We have demonstrated an optimized design for a QCL without injector by introducing AIAs barriers and InAs-containing quantum wells in the active region. All device-relevant parameters are significantly enhanced. The laser with the modified active region, a doping of  $2.6 \times 10^{16} \text{ cm}^{-3}$  and an HR coating has a record low threshold current density of 450  $\text{A}/\text{cm}^2$  measured in the pulsed mode at 300 K. Furthermore, this device showed a maximum operating temperature of 410 K, a slope efficiency of 700  $\text{mA}/\text{W}$ , a front facet wall plug efficiency of 2% and a characteristic temperature of 140 K. These values are comparable to those of other mid-infrared QCLs using injectors [6,7] and regarding threshold performance even exceed them.

#### Acknowledgement

We gratefully acknowledge the support of the Nano Initiative Munich NIM.

#### References

- [1] Wanke, et al., Appl. Phys. Lett. 78 (25) (2001) 3950.
- [2] Friedrich, et al., Electron. Lett. 42 (2006) 21.
- [3] Katz, et al., Electron. Lett. 44 (2008) 580.
- [4] Friedrich, et al., Semicond. Sci. Technol. 22 (2007) 218.
- [5] Semtsiv, et al., Appl. Phys. Lett. 89 (2006) 211124.
- [6] Wang, et al., Appl. Phys. Lett. 90 (2007) 211103.
- [7] Slivken, et al., Appl. Phys. Lett. 90 (2007) 151115.